ELSEVIER

Neurobiology of Aging 32 (2011) S48–S57

NEUROBIOLOGY OF AGING

www.elsevier.com/locate/neuaging

Alliance for Aging Research AD Biomarkers Work Group: structural MRI

Clifford R. Jack, Jr.

Mayo Foundation, Rochester, MN, USA

Abstract

Biomarkers of Alzheimer's disease (AD) are increasingly important. All modern AD therapeutic trials employ AD biomarkers in some capacity. In addition, AD biomarkers are an essential component of recently updated diagnostic criteria for AD from the National Institute on Aging—Alzheimer's Association. Biomarkers serve as proxies for specific pathophysiological features of disease. The 5 most well established AD biomarkers include both brain imaging and cerebrospinal fluid (CSF) measures—cerebrospinal fluid Abeta and tau, amyloid positron emission tomography (PET), fluorodeoxyglucose (FDG) positron emission tomography, and structural magnetic resonance imaging (MRI). This article reviews evidence supporting the position that MRI is a biomarker of neurodegenerative atrophy. Topics covered include methods of extracting quantitative and semiquantitative information from structural MRI; imaging-autopsy correlation; and evidence supporting diagnostic and prognostic value of MRI measures. Finally, the place of MRI in a hypothetical model of temporal ordering of AD biomarkers is reviewed.

Keywords: Alzheimer's disease; Biomarkers; MRI

1. How are measures of neurodegenerative atrophy extracted from structural MRI images?

The topographic pattern of neurodegenerative atrophy in Alzheimer's disease (AD) captured by anatomic magnetic resonance imaging (MRI) mirrors that of neurofibrillary pathology (Braak and Braak, 1991; Whitwell et al., 2007, 2008a). Atrophy begins in and is ultimately most severe in the medial temporal lobe, particularly the entorhinal cortex and hippocampus, which is why these structures have been targeted in many MRI studies for diagnostic purposes. Atrophy later spreads to the inferior temporal lobe and paralimbic cortical areas. The transition from mild cognitive impairment (MCI) to full dementia is felt to be due to spread of degenerative atrophy to multimodal association neocortices. Below is a brief survey of methods to extract and/or visualize this information from 3-D MRI scans of cross-sectional and longitudinal studies (modified from Vemuri and Jack, 2010).

1.1. Cross-sectional methods

1.1.1. Visual assessment of scans

Visual assessment of the degree of atrophy in the medial temporal lobe is often used to assess disease severity and to add confidence in a clinical diagnosis of AD (Scheltens et al., 1992). Fig. 1 shows the medial temporal lobe in cognitively normal elderly (CN), amnestic mild cognitive impairment (aMCI), and AD. While simple visual assessment is easily implemented and widely available, atrophy is a continuous process and this method does not lend itself to accurate or reproducible assessment of fine incremental grades of atrophy.

1.1.2. Quantitative ROI-based techniques

Manual tracing and quantifying the volume of medial temporal lobe structures, e.g., the hippocampus or entorhinal cortex has been traditionally employed and provides an accurate quantitative measure of atrophy but is time-consuming (Fox et al., 1996; Jack et al., 1992).

Corresponding author at: Mayo Foundation, 200 1st Street SW, Rochester, MN 55905, USA. Tel.: 507-284-8548.

E-mail address: jack.clifford@mayo.edu (C.R. Jack, Jr.).

0197-4580/$ – see front matter © 2011 Published by Elsevier Inc.
doi:10.1016/j.neurobiolaging.2011.09.011

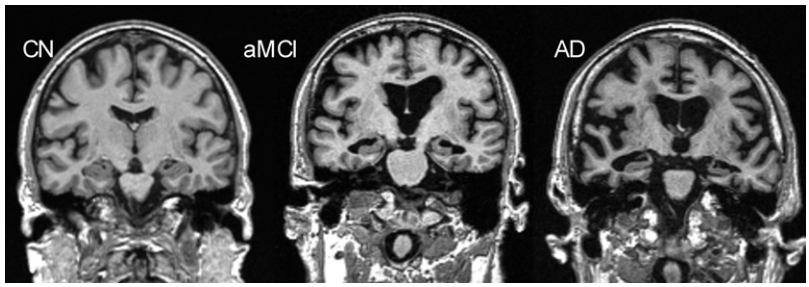

Fig. 1. Progressive atrophy (especially medial temporal lobes) in elderly cognitively normal (CN), amnestic mild cognitive impairment (aMCI), and Alzheimer's disease (AD) subjects.

1.1.3. Automated and semiautomated techniques

Methods have been developed to automatically parcellate gray matter density (Tzourio-Mazoyer et al., 2002) or the thickness of cortical surfaces (Dale et al., 1999; Fischl et al., 2004) into regions of interest. This is computationally intensive but is reproducible and does not require manual intervention.

An advantage of measuring something like the hippocampus is that the measurements describe a known anatomic structure that (in the case of the hippocampus) is closely related to the pathological expression of the disease and is also functionally related to 1 of the cardinal early clinical symptoms—memory impairment. The disadvantage of using a single structure or region of interest (ROI) to consolidate 3-D information is that it is topographically limited and does not make use of all the available information in a 3-D MRI.

1.1.4. Quantitative voxel-based

These methods assess atrophy over the entire 3-D MRI scan.

1.1.1.4. Voxel-based analytic techniques. Methods such as voxel-based morphometry (VBM) (Ashburner and Friston, 2000) are a popular and useful way to test for group-wise differences in the topography of atrophy. However, the statistical testing portion of voxel-based morphometry is not designed to provide diagnostic information at the single subject level.

1.1.4.2. Automated individual subject diagnosis. Several investigators have developed multivariate analysis and machine learning-based algorithms which use the entire 3-D MRI data to form a disease model against which individual subjects may be compared. A new incoming scan is scored based on the degree and the pattern of atrophy in comparison with the scans of a large database of well characterized subjects (Alexander and Moeller, 1994; Csernansky et al., 2000; Davatzikos et al., 2009; Fan et al., 2005; Kloppel et al., 2008; Stonnington et al., 2008; Vemuri et al., 2008a; Welch et al., 2002). Such measures capture the severity of neuronal pathology, i.e., Braak staging, better than hippocampal volumes (Vemuri et al., 2008b).

1.2. Longitudinal methods

While change over time can be determined by simply measuring a volume independently on each scan in a series and performing arithmetic subtraction of the volumes, more sophisticated techniques have been developed to extract tissue loss information from serial MRI scans. In these techniques all MRI scans within a subject's time series are registered to each other and brain loss between scans is quantified as a measure of neurodegenerative disease progression.

1.2.1. Global atrophy quantification

One of the earliest methods developed to quantify the global change in brain volume between 2 scans was the boundary shift integral (BSI) (Fox and Freeborough, 1997; Freeborough and Fox, 1997). BSI determines the total volume through which the surface of the brain has moved between scans acquired at 2 time points, i.e., as the brain volume decreases and the volume of the ventricles increases.

1.2.2. Tensor-based morphometry (TBM)

Unlike BSI which only analyzes spatial shift in the brain surfaces, TBM provides 3-D patterns of voxel-level brain degeneration (Chételat et al., 2005; Thompson and Apostolova, 2007).

2. Evidence validating MRI as a neurodegenerative biomarker in AD

Evidence validating MRI as a neurodegenerative AD biomarker is reviewed below. Studies are classified on several criteria, including the method of measurement, numbers of subjects, and source of subjects. The ideal source is an epidemiological or population-based cohort. The next best option is a community-based sample. The least desirable but most common source of data are referral samples, which have the highest risk of biases. Evidence validating MRI as an AD biomarker takes the form of several different types of studies: cross-sectional clinical-MRI correlations; prediction of future clinical change; correlating change-over-time on serial MRI with concurrent change on clinical indexes; and MRI-autopsy correlation.

Table 1
Cross sectional separation of clinically diagnosed AD versus controls

Study	Subjects	Source of subjects	Measurement method	Results
Desikan et al., 2009	CN 94, AD 65	Referral sample	Ctx thickness, ERC + Hipp + SupMarg gyrus	AUROC 1.0
Gerardin et al., 2009	CN 25, AD 23	Referral sample ADNI	Hippocampal shape metric	Sensitivity 96%, specificity 92%
Hinrichs et al., 2009	CN 94, AD 89	Referral sample ADNI	Multi voxel classifier	AUROC 0.88
Jack et al., 1992	CN 22, AD 20	Community sample	Manual hippocampal volume adjusted for head size and age	Sensitivity 95%, specificity 95%, accuracy 89%, AUROC 0.92
Killiany et al., 2000	CN 24, AD 16	Referral sample	ERC, banks of superior temp sulcus, anterior cingulate	Accuracy 100%
Kohannim et al., 2010	CN 213, AD 158	Referral sample ADNI	Multi voxel classifier	AUROC 0.89
McEvoy et al., 2009	CN 139, AD 84	Referral sample ADNI	Ct thickness; medial and lateral temporal, isthmus cingulated orbitofrontal	Sensitivity 83%, specificity 93%
Walhovd et al., 2010	42 CN, 38 AD	Referral sample ADNI	Ct thickness	Accuracy 85%

Key: AD, Alzheimer's disease; ADNI, Alzheimer's Disease Neuroimaging Initiative; AUROC, area under receiver operating characteristic curve; CN, cognitively normal.

2.1. Cross-sectional clinical-MRI correlations

Many studies have been published describing the accuracy, sensitivity, specificity, or area under receiver operating characteristic curve (AUROC) with which clinically diagnosed AD subjects can be separated from cognitively normal elderly control subjects. This is the simplest type of data to acquire and hence this is the most frequent type of study found in the literature. This is the weakest category of validation data, because the gold standard against which the MRI is compared is a clinical diagnosis, which can be wrong. A clinical diagnosis is also available in the absence of any biomarker data. Accuracy ranges from 85% to 100%. Different methods have been employed as described above. The literature is too vast to describe each publication, but Table 1 contains some representative examples of studies demonstrating cross-sectional separation of clinically diagnosed AD versus controls. Results vary depending on measurement method, source of subjects, and statistical endpoints.

A related class of studies is those that demonstrate cross-sectional separation of clinically diagnosed controls versus subjects with mild cognitive impairment. Mild cognitive impairment may have been defined using the formal diagnostic criteria for MCI outlined by Petersen (2004) or may have been defined using other criteria. Table 2 contains some representative examples of studies demonstrating cross-sectional separation of clinically diagnosed controls versus subjects with mild cognitive impairment using quantitative MRI measures. Results vary depending on measurement method, source of subjects, and statistical endpoints.

2.2. Autopsy-MRI correlation

MRI-autopsy studies have convincingly validated that quantitative measurements of brain volume loss correlate with pathological indexes of neurodegenerative severity. Hippocampal volumes measured from antemortem MRI scans correlate with Braak neurofibrillary tangle pathologic staging in both demented and nondemented subjects (Gosche et al., 2002; Jack et al., 2002). Antemortem hippocampal volume as well as rates of brain and hippocampal atrophy from MRI correlate with hippocampal neurofibrillary tangle density (Csernansky et al., 2004; Silbert et al., 2003) at autopsy. Excellent correlation is found between hippocampal volume measures obtained on either antemortem MRI (Zarow et al., 2005) or postmortem MRI (Bobinski et al., 2000) and hippocampal neuron cell counts in autopsy specimens. On the basis of these imaging-to-pathology correlation studies, quantitative measures from structural MRI, such as hippocampal volume, are inferred to represent an approximate surrogate of the stage/severity of neuronal pathology—neuron loss, neuron shrinkage, and synapse loss—that occurs in AD. Voxel-wise studies of gray matter

Table 2
Cross-sectional separation of clinically diagnosed mild cognitive impairment versus controls

Study	Subjects	Source of subjects	Measurement method	Results
Desikan et al., 2009	CN 94, MCI 57	Referral sample	Ctx thickness of ERC + Hipp + SupMarg gyrus	AUROC 0.95, sensitivity 90%, specificity 91%
Gerardin et al., 2009	CN 25, MCI 23	Referral sample ADNI	Hippocampal shape metric	Sensitivity 83%, specificity 84%
Kohannim et al., 2010	CN 213, MCI 264	Referral sample ADNI	Multi voxel classifier	AUROC 0.84
Xu et al., 2000	CN 30, MCI 30	Community sample	Hippocampal W score	Sensitivity 63%, specificity 80%

Key: ADNI, Alzheimer's Disease Neuroimaging Initiative; AUROC, area under receiver operating characteristic curve.

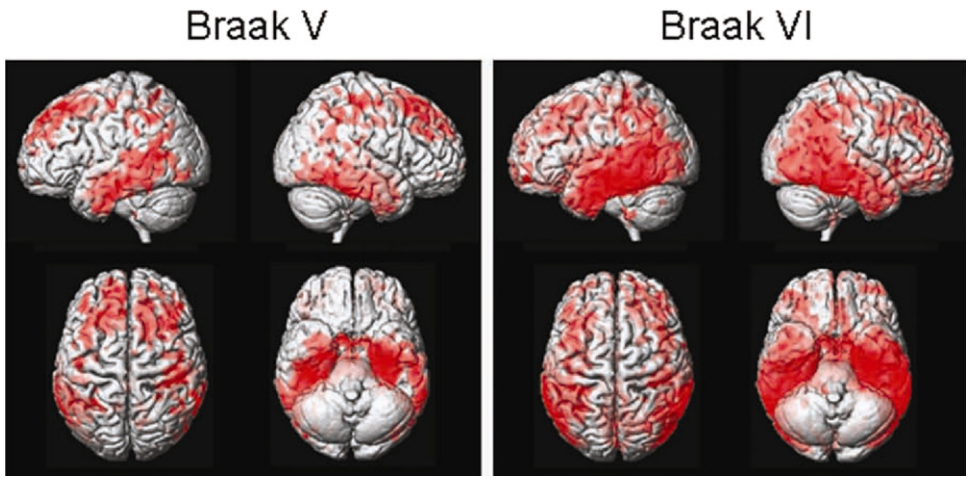

Fig. 2. Topography of gray matter loss versus Braak stage.

loss demonstrate that the topographic distribution of gray matter loss closely mirrors Braak and Braak spatial distribution of neurofibrillary pathology in subjects who have had antemortem MRI and have come to autopsy (Fig. 2) (Whitwell et al., 2008). Fully automated multivoxel analysis methods demonstrate close correlation between quantitative antemortem MRI and Braak staging, as depicted in Fig. 3 with STructural Abnormality iNDex (STAND) scores.

We point out that while MRI measures of atrophy do scale with pathological indexes of neurodegeneration, brain atrophy is not specific for AD. It occurs in other conditions that may be associated with cognitive impairment, such as cerebrovascular disease, hippocampal sclerosis, frontal temporal lobar degeneration, and head trauma (Jack et al., 2002; Jagust et al., 2008; Zarow et al., 2005).

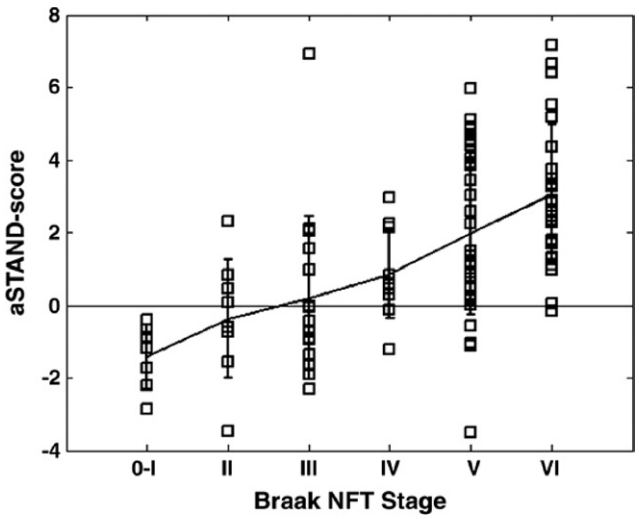

Fig. 3. MRI STructural Abnormality iNDex (STAND) score versus Braak stage.

3. Modeling of the longitudinal trajectory of AD with biomarkers—where does structural MRI fit?

Because different AD biomarkers provide information about different AD-related pathological processes, it stands to reason that comprehensive in vivo assessment of the disease requires information from different classes of biomarkers. Based on the assumptions that MRI provides an index of neurodegenerative pathologic burden (above) and Pittsburgh Compound B (PIB) positron emission tomography (PET) a measure of amyloid plaque burden, a model of AD has been proposed in which the rate of amyloid deposition and the rate of neurodegeneration later in life are dissociated. The presence of brain amyloidosis is necessary but not sufficient to produce cognitive decline; the neurodegenerative component of AD pathology is the immediate substrate of cognitive impairment, and the rate of cognitive decline is driven by the rate of neurodegeneration. In this proposed model, amyloid deposition is dynamic early in the disease process (presymptomatically) while neurodegeneration is dynamic in the mid- to late-stage. This amyloid and neurodegeneration model (Jack et al., 2009) is reproduced in Fig. 4. In the model, the lifetime course of the disease is divided into clinically defined presymptomatic, early symptomatic (MCI), and dementia phases. Neurodegeneration, detected by atrophy on volumetric MRI, is indicated by a dashed line. Cognitive function is indicated by a dot-dash line. Amyloid deposition, detected by PIB, is indicated by a solid line later in the course of AD (i.e., that portion of the disease for which PIB data are now available). The time course of amyloid deposition early in life is represented as 2 possible theoretical trajectories (dotted lines), reflecting uncertainty about the time course of early PIB signal.

An expanded version of this disease biomarker model (Jack et al., 2010a) incorporates the 5 most well validated AD biomarkers into a comprehensive sequence of pathological events as subjects progress from cognitively normal

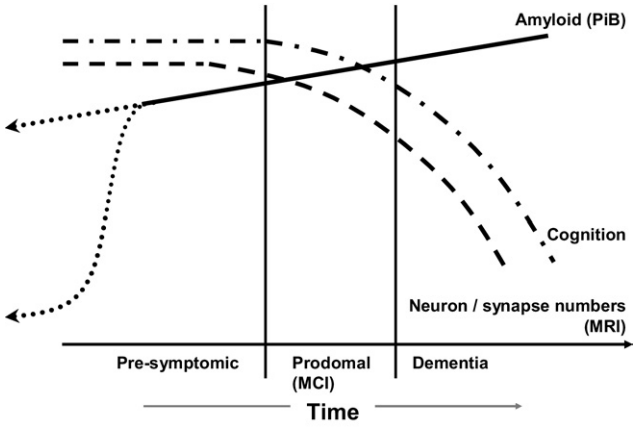

Fig. 4. Amyloid and neurodegeneration model. Abbreviations: PIB, Pittsburgh Compound B; MCI, mild cognitive impairment; MRI, magnetic resonance imaging. Modified from Jack et al., 2009.

in middle age to dementia in older age. There are presently 5 well-accepted biomarkers of AD. Both cerebrospinal fluid (CSF) Aβ42 and amyloid PET imaging are biomarkers of Aβ plaque deposition. CSF tau is an indicator of tau pathology and associated neuronal injury. Fluorodeoxyglucose (FDG) PET measures AD-mediated neuronal dysfunction, while structural MRI measures AD-mediated neurodegeneration. This model rests on the assumption that these 5 AD biomarkers become abnormal in a sequential manner, but their time courses also overlap. The hypothesis is that amyloid PET imaging and CSF Aβ42 become abnormal first, perhaps as much as 20 years before the first clinical symptoms appear. CSF tau and FDG PET become abnormal later and structural MRI is the last of the 5 major biomarkers to become abnormal. CSF tau, FDG PET, and structural MRI correlate with clinical symptom severity while CSF Aβ42 and amyloid PET imaging may not. The hypothesis is that together these 5 biomarkers of AD are able to stage the complete trajectory of AD, which may span as much as 20–30 years or more in affected individuals. Fig. 5 illustrates this expanded model (Jack et al., 2010a).

4. Use of MRI in therapeutic trials

MRI is used in several different ways in therapeutic trials. Therapeutic modification of the natural rate of atrophy has been used as an outcome measure in a number of AD and MCI trials. As a measure of the severity or stage of neurodegeneration, MRI has been used as a covariate in analyses, much the same way disease severity on clinical scales like the Mini Mental State Examination (MMSE) or AD Assessment Scale—Cognitive (ADAS—Cog) is used. In theory MRI can also be used to stratify trial subjects at baseline on the basis of disease severity. Although the discussion above has focused on structural MRI as a measure of the severity of AD-related neurodegeneration, MRI also is commonly used for inclusion/exclusion purposes in therapeutic trials. For example, hemispheric cerebral infarction, tumor, normal pressure hydrocephalus (NPH), prior surgery, major head trauma, and cerebral hemorrhage are common exclusionary findings on screening MRI. Micro hemorrhages that exceed a prespecified number are also a common exclusionary finding in antiamyloid trials. The major barrier to the use of volumetric MRI as an outcome measure in clinical trials has been lack of standardization of MRI methods, particularly methods for extracting quantitative information from scans. This lack of standardization leads to different results (Tables 1–4), which in turn undermines the credibility of the method in the minds of regulators. Although initiatives such as the Alzheimer's Disease Neuroimaging Initiative (ADNI) have focused on standard-

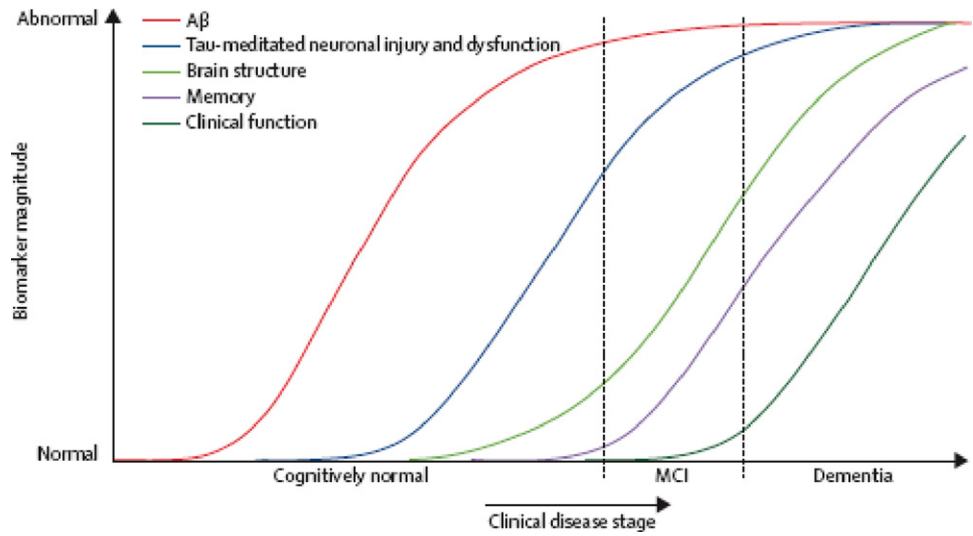

Fig. 5. Expanded model with 5 biomarkers. Aβ, amyloid-beta; MCI, mild cognitive impairment. Modified from Jack et al., 2010a.

Table 3
Predicting progression from mild cognitive impairment to AD

Study	Subjects	Source of subjects	Measurement method	Results
Bakkour et al., 2009	49 CDR 0.5	Referral sample	Cortical thickness in temporal and parietal ROIs	Predict MCI progression to AD, 83% sensitivity and 65% specificity
Brys et al., 2009	24 MCI	Referral sample	Medial temporal lobe gray matter concentration	Accuracy, predict MCI progression to AD: 74%
Convit et al., 2000	46 Normal or MCI	Referral sample	Hippocampal volume	Declining subjects had 11.3% of reduction in HC compared with nondecliners
DeCarli et al., 2007	190 MCI	ADCS Vit E donepezil trial	Visual assessment of hippocampal atrophy	Atrophy score $>$ 2.0 increased likelihood of progression, HR: 2.30
Desikan et al., 2009	129 MCI	Referral sample ADNI	Hippocampal volume	Predict MCI progression to AD, adjusted HR: 0.73 (0.51–1.04)
Desikan et al., 2008	47 MCI	Referral sample	Temporal-parietal regions of interest	Combination of entorhinal cortex (HR = 0.60) and the inferior parietal lobule (HR = 0.62) was best predictor of time to progression to AD
Devanand et al., 2007	139 MCI	Referral sample	Hippocampal volume	Predict MCI progression to AD, HR: 2.84 (1.47–5.49)
Eckerström et al., 2008	42 MCI	Referral sample	Hippocampal volume	Hippocampal volumes smaller in converters to AD versus nonconverters
Fleisher et al., 2008	129 aMCI	ADCS Vit E donepezil trial	Ventricular volumes and hippocampal volumes	Ventricular volumes and hippocampal volumes predicted progression to AD
Galluzzi et al., 2010	90 MCI	Referral sample	Medial temporal atrophy	Predict MCI progression to AD, AUC: 0.73
Galton et al., 2005	31 CDR 0.5	Referral sample	Hippocampal volume	Converters had a greater atrophy compared with nonconverters.
Henneman et al., 2009	39 MCI	Referral sample	Hippocampal volume adjusted for age, sex, baseline MMSE	Predict MCI progression to AD, HR: 10.4 (3.1–34.8)
Herukka et al., 2008	21 MCI	Referral sample	Hippocampal volume	Predict MCI progression to AD, right HC: 15.8 (1.4–174.2)
Jack et al., 2010b	218 MCI	ADNI plus Mayo community sample	Hippocampal volume	Predict MCI progression to AD, HR 2.6 (1.8–3.8) 25% versus 75%
Jack et al., 2008	131 MCI	ADCS Vit E donepezil trial	Volumes of hippocampus, entorhinal cortex, brain, ventricle	Rates of change in all volumes were greater in converters than nonconverters
Jack et al., 2005	72 MCI	Community sample	Hippocampal volume	Predict MCI progression to AD, HC volume OR: 1.51 (1.1–2.0)
Jack et al., 2000	43 MCI	Community sample	Hippocampal volume	Rates of hippocampal atrophy were greater in converters than nonconverters
Jack et al., 1999	80 MCI	Community sample	Hippocampal W score	Relative risk 0.69—for each 1 unit increase in W score (less atrophy) risk of progression to AD decreased by 31%
Kantarci et al., 2005	21 MCI	Referral sample	Hippocampal volume	Predict MCI progression to AD OR: 2.5 (1.0–6.2)
Killiany et al., 2002	94 CDR 0.5	Referral sample	Hippocampal volume	Predict MCI progression to AD OR: 1.5 (1.0–2.31)
Landau et al., 2010	85 MCI	Referral sample	Hippocampal volume	Predict MCI progression to AD OR: 2.49 (1.02–5.96)
Leung et al., 2010	335 MCI	ADNI	Hippocampal volume	Rates higher in converters compared with stable and reverter groups
Risacher et al., 2009	227 MCI	ADNI	Hippocampal volume	Effect size for separating MCI stable versus converter Cohen's d = 0.60
Stoub et al., 2010	29 aMCI	Referral sample	Entorhinal cortex and hippocampus	Atrophy rate of entorhinal cortex and hippocampus in controls less than MCI converters
Tapiola et al., 2008	60 MCI	Referral sample	Hippocampal volume	Predict MCI progression to AD OR: total HC 0.815 (0.69–0.97)
Vemuri et al., 2009	192 MCI	Referral sample ADNI	STAND score	HR for time to conversion from MCI to AD 25th versus 75th percentile 2.6
Visser et al., 1999	13 MCI	Community sample	Hippocampal volume	Predict MCI progression to AD OR: 0.21 (0.05–0.99)
Visser et al., 2002	30 MCI	Community sample	Hippocampal volume	Hippocampal volume predicts MCI progression to AD
Wang et al., 2009	58 aMCI	Referral sample	Hippocampal volume	Predict MCI progression to AD left HC HR: 0.38 (0.10–0.88)

Key: AD, Alzheimer's disease; ADNI, Alzheimer's Disease Neuroimaging Initiative; aMCI, amnestic mild cognitive impairment; AUC, area under the curve; CDR, Clinical Dementia Rating; HR, hazard ratio; MCI, mild cognitive impairment; MMSE, Mini Mental State Examination; OR, odds ratio; ROIs, regions of interest; STAND, STructural Abnormality iNDex;

izing imaging methods, to date universally accepted standards for MRI image quantification have not emerged.

At the present time, AD biomarkers have not yet been validated as surrogate endpoints for regulatory purposes. However the impact of interventions on these biomarkers has been evaluated in a few trials and was found to be potentially useful in capturing the pharmacodynamic effects of an agent. The efficacy of donepezil, an acetylcholinesterase inhibitor, was evaluated using serial anatomic MRI (Hashimoto et al., 2005; Jack et al., 2008; Krishnan et al., 2003) and was found to possibly be neuroprotective based on some evidence of decreased rates of atrophy in the treatment versus placebo arms. In a different study, antibody responders immunized to amyloid-beta (A) had more rapid volume loss than placebo patients during a Phase IIa immunotherapy trial that was prematurely terminated due to meningoencephalitis in a small subset of patients (Fox et al., 2005).

5. Predicting the risk of progression in MCI and CN

About 12%–15% of MCI subjects annually progress to AD (Fischer et al., 2007; Petersen, 2007); however, clinical criteria alone cannot identify with certainty which subjects will progress more rapidly than others. For this reason, predictive information from imaging has been sought to supplement clinical prognostic indicators. Studies demonstrating the ability of MRI to predict future progression have taken several forms. Studies using time-to-event methods are appropriate when follow-up times vary among subjects in the cohort which is most commonly the case. Such studies typically employ Cox proportional hazards models in which cutoffs stratify a baseline MRI measurement into risk groups and the results are reported as hazard ratios (HR) (Jack et al., 1999). This type of analysis relates an imaging measurement to the time to progression from a diagnosis of MCI to AD, not to the lifetime risk of developing AD. A related method of analysis employs a rate of change at baseline as the predictor rather than a brain volume measurement at 1 point in time (Jack et al., 2005). If all subjects in the study have the same follow-up time, then simply comparing baseline MRI between progressors and nonprogressors is appropriate. Unfortunately, several studies have simply compared baseline MRI measures between progressors and nonprogressors when follow-up times were not the same across subjects in the cohort. Inferences about imaging as a predictor may be invalid in this situation because subjects classified as progressors may simply be those who have longer follow-up times than subjects classified as nonprogressors. Table 3 illustrates examples of studies evaluating the ability of baseline MRI measures to predict time to progression from MCI to AD. Results vary depending on measurement method, source of subjects, and statistical endpoints.

Table 4
Sample sizes per arm needed to power treatment study in AD/MCI

Citation	Subjects	Source of subjects	Measurement method	Sample size required to detect treatment effects
Fox et al., 2000	18 AD	Referral sample	Classic BSI	207 per arm assuming: 1-year trial, 20% effect size, 90% power, 10% dropout, 10% unusable scans
Holland et al., 2009	129 AD;299 MCI	Referral sample ADNI	Ctx thickness ERC ROI	Assuming 24-mo trial, 25% effect size, 80% power, scans every 6 mo ;45 per arm for AD; 135 per arm MCI
Hua et al., 2010	50 AD;MCI 122	Referral sample ADNI	TBM temporal lobe	Assuming 12-mo trial, 25% effect size, 80% power; 43 AD per arm; 82 MCI per arm
Jack et al., 2003	192 AD	Referral sample, terminated multisite therapeutic trial	Hippocampus	Assuming 12-mo trial, 50% effect size, 90% power at 0.05; 21 per arm for AD
Leung et al., 2010	81 AD	Referral sample ADNI	KN-BSI	Assuming 12-mo trial, 25% effect size, 80% power; 81 AD per arm
Schott et al., 2006	46 AD	Referral sample	BSI	Assuming 12-mo trial, 20% effect size, 90% power, 2-sided significance at 0.05, 4 ideally spaced scans; 138 AD per arm
Schuff et al., 2009	96 AD;226 MCI	Referral sample ADNI	Hippocampal volume (SNT), model includes 3 scans, Markov chain, APOE	Assuming 12-mo trial, 25% effect size, 90% power; 186 AD per arm; 341 MCI per arm
Vemuri et al., 2010	71 AD;149 MCI	Referral sample ADNI	Ventricular-BSI	Assuming 12-mo trial, 25% effect size, 80% power, 2-sided 2 sample *t* test at 0.05; 100 AD per arm; 186 MCI per arm
Wolz et al., 2010	126 AD;279 MCI	Referral sample ADNI	Simultaneous 4-D graph segmentation	Assuming 12-mo trial, 25% effect size, 80% power, 2-sided 2 sample *t* test at 0.05; 67 AD per arm; 206 MCI per arm

Key: AD, Alzheimer's disease; ADNI, Alzheimer's Disease Neuroimaging Initiative; APOE, apolipoprotein E; BSI, boundary shift integral; MCI, mild cognitive impairment; ROI, region of interest; TBM, tensor-based morphometry.

6. Measuring longitudinal disease progression with serial MRI scans

The idea of using change-over-time measures of brain volume on serial MRI was introduced by Freeborough and Fox (1997). This approach has appeal as a means of measuring disease progression that is independent of clinical assessment. It has found utility in assessments of individual subjects; in longitudinal observational studies; and as an outcome measurement in therapeutic trials. The potential of change-over-time measures as outcomes in therapeutic trials is particularly appealing because longitudinal MRI measures have considerably better precision and therefore can be powered with much smaller sample sizes than traditional clinical assessment tools. A number of different methodological approaches have been employed ranging from simple manual tracing to sophisticated TBM methods. Several investigators have shown that the lower variance in the serial MRI measurements compared with clinical measures of cognition and function could potentially permit performing clinical trials with smaller sample sizes than would be possible using traditional clinical instruments (Fox et al., 2000; Hua et al., 2008; Jack et al., 2003; Schott et al., 2006; Vemuri et al., 2010). Table 4 illustrates examples of sample sizes needed to power AD or MCI trials. Results vary depending on measurement method, assumptions about the trial design, and statistical methods.

Conflict of interest statement

The author has no relevant conflicts.

References

Alexander, G.E., Moeller, J.R., 1994. Application of the scaled subprofile model to functional imaging in neuropsychiatric disorders: a principal component approach to modeling regional patterns of brain function in disease. Hum. Brain Mapp. 2, 79–94.

Ashburner, J., Friston, K.J., 2000. Voxel-based morphometry—the methods. Neuroimage 11, 805–821.

Bakkour, A., Morris, J.C., Dickerson, B.C., 2009. The cortical signature of prodromal AD: regional thinning predicts mild AD dementia. Neurology 72, 1048–1055.

Bobinski, M., de Leon, M.J., Wegiel, J., Desanti, S., Convit, A., Saint Louis, L.A., Rusinek, H., Wisniewski, H.M., 2000. The histological validation of post mortem magnetic resonance imaging-determined hippocampal volume in Alzheimer's disease. Neuroscience 95, 721–725.

Braak, H., Braak, E., 1991. Neuropathological stageing of Alzheimer-related changes. Acta Neuropathol. 82, 239–259.

Brys, M., Glodzik, L., Mosconi, L., Switalski, R., De Santi, S., Pirraglia, E., Rich, K., Kim, B.C., Mehta, P., Zinkowski, R., Pratico, D., Wallin, A., Zetterberg, H., Tsui, W.H., Rusinek, H., Blennow, K., de Leon, M.J., 2009. Magnetic resonance imaging improves cerebrospinal fluid biomarkers in the early detection of Alzheimer's disease. J. Alzheimers Dis. 16, 351–362.

Chételat, G., Landeau, B., Eustache, F., Mézenge, F., Viader, F., de la Sayette, V., Desgranges, B., Baron, J.C., 2005. Using voxel-based morphometry to map the structural changes associated with rapid conversion in MCI: a longitudinal MRI study. Neuroimage 27, 934–946.

Convit, A., de Asis, J., de Leon, M.J., Tarshish, C.Y., De Santi, S., Rusinek, H., 2000. Atrophy of the medial occipitotemporal, inferior, and middle temporal gyri in non-demented elderly predict decline to Alzheimer's disease. Neurobiol. Aging 21, 19–26.

Csernansky, J.G., Hamstra, J., Wang, L., McKeel, D., Price, J.L., Gado, M., Morris, J.C., 2004. Correlations between antemortem hippocampal volume and postmortem neuropathology in AD subjects. Alzheimer Dis. Assoc. Disord. 18, 190–195.

Csernansky, J.G., Wang, L., Joshi, S., Miller, J.P., Gado, M., Kido, D., McKeel, D., Morris, J.C., Miller, M.I., 2000. Early DAT is distinguished from aging by high-dimensional mapping of the hippocampus. Dementia of the Alzheimer type. Neurology 55, 1636–1643.

Dale, A.M., Fischl, B., Sereno, M.I., 1999. Cortical surface-based analysis. I. Segmentation and surface reconstruction. Neuroimage 9, 179–194.

Davatzikos, C., Xu, F., An, Y., Fan, Y., Resnick, S.M., 2009. Longitudinal progression of Alzheimer's-like patterns of atrophy in normal older adults: the SPARE-AD index. Brain 132, 2026–2035.

DeCarli, C., Frisoni, G.B., Clark, C.M., Harvey, D., Grundman, M., Petersen, R.C., Thal, L.J., Jin, S., Jack, C.R., Jr., Scheltens, P., Alzheimer's Disease Cooperative Study Group, 2007. Qualitative estimates of medial temporal atrophy as a predictor of progression from mild cognitive impairment to dementia. Arch. Neurol. 64, 108–115.

Desikan, R.S., Cabral, H.J., Hess, C.P., Dillon, W.P., Glastonbury, C.M., Weiner, M.W., Schmansky, N.J., Greve, D.N., Salat, D.H., Buckner, R.L., Fischl, B., 2009. Automated MRI measures identify individuals with mild cognitive impairment and Alzheimer's disease. Brain 132, 2048–2057.

Desikan, R.S., Fischl, B., Cabral, H.J., Kemper, T.L., Guttmann, C.R., Blacker, D., Hyman, B.T., Albert, M.S., Killiany, R.J., 2008. MRI measures of temporoparietal regions show differential rates of atrophy during prodromal. Adv. Neurol. 71, 819–825.

Devanand, D.P., Pradhaban, G., Liu, X., Khandji, A., De Santi, S., Segal, S., Rusinek, H., Pelton, G.H., Honig, L.S., Mayeux, R., Stern, Y., Tabert, M.H., de Leon, M.J., 2007. Hippocampal and entorhinal atrophy in mild cognitive impairment: prediction of Alzheimer disease. Neurology 68, 828–836.

Eckerström, C., Olsson, E., Borga, M., Ekholm, S., Ribbelin, S., Rolstad, S., Starck, G., Edman, A., Wallin, A., Malmgren, H., 2008. Small baseline volume of left hippocampus is associated with subsequent conversion of MCI into dementia: the Göteborg MCI study. J. Neurol. Sci. 272, 48–59.

Fan, Y., Shen, D., Davatzikos, C., 2005. Classification of structural images via high-dimensional image warping, robust feature extraction, and SVM. Med. Image Comput. Comput. Assist. Interv.. 8, 1–8.

Fischer, P., Jungwirth, S., Zehetmayer, S., Weissgram, S., Hoenigschnabl, S., Gelpi, E., Krampla, W., Tragl, K.H., 2007. Conversion from subtypes of mild cognitive impairment to Alzheimer dementia. Neurology 68, 288–291.

Fischl, B., van der Kouwe, A., Destrieux, C., Halgren, E., Ségonne, F., Salat, D.H., Busa, E., Seidman, L.J., Goldstein, J., Kennedy, D., Caviness, V., Makris, N., Rosen, B., Dale, A.M., 2004. Automatically parcellating the human cerebral cortex. Cereb. Cortex 14, 11–22.

Fleisher, A.S., Sun, S., Taylor, C., Ward, C.P., Gamst, A.C., Petersen, R.C., Jack, C.R., Jr., Aisen, P.S., Thal, L.J., 2008. Volumetric MRI vs clinical predictors of Alzheimer disease in mild cognitive impairment. Neurology 70, 191–199.

Fox, N.C., Black, R.S., Gilman, S., Rossor, M.N., Griffith, S.G., Jenkins, L., Koller, M., AN1792(QS-21)-201 Study Team, 2005. Effects of Abeta immunization (AN1792) on MRI measures of cerebral volume in Alzheimer disease. Neurology 64, 1563–1572.

Fox, N.C., Cousens, S., Scahill, R., Harvey, R.J., Rossor, M.N., 2000. Using serial registered brain magnetic resonance imaging to measure disease progression in Alzheimer disease: power calculations and estimates of sample size to detect treatment effects. Arch. Neurol. 57, 339–344.

Fox, N.C., Freeborough, P.A., 1997. Brain atrophy progression measured from registered serial MRI: validation and application to Alzheimer's disease. J. Magn. Reson. Imaging 7, 1069–1075.

Fox, N.C., Freeborough, P.A., Rossor, M.N., 1996. Visualisation and quantification of rates of atrophy in Alzheimer's disease. Lancet 348, 94–97.

Freeborough, P.A., Fox, N.C., 1997. The boundary shift integral: an accurate and robust measure of cerebral volume changes from registered repeat MRI. IEEE Trans. Med. Imaging 16, 623–629.

Galluzzi, S., Geroldi, C., Ghidoni, R., Paghera, B., Amicucci, G., Bonetti, M., Zanetti, O., Cotelli, M., Gennarelli, M., Frisoni, G.B., Translational Outpatient Memory Clinic Working Group, 2010. The new Alzheimer's criteria in a naturalistic series of patients with mild cognitive impairment. J. Neurol. 257, 2004–2014.

Galton, C.J., Erzinçlioglu, S., Sahakian, B.J., Antoun, N., Hodges, J.R., 2005. A comparison of the Addenbrooke's Cognitive Examination (ACE), conventional neuropsychological assessment, and simple MRI-based medial temporal lobe evaluation in the early diagnosis of Alzheimer's disease. Cogn. Behav. Neurol. 18, 144–150.

Gerardin, E., Chételat, G., Chupin, M., Cuingnet, R., Desgranges, B., Kim, H.S., Niethammer, M., Dubois, B., Lehéricy, S., Garnero, L., Eustache, F., Colliot, O., Alzheimer's Disease Neuroimaging Initiative, 2009. Multidimensional classification of hippocampal shape features discriminates Alzheimer's disease and mild cognitive impairment from normal aging. Neuroimage 47, 1476–1486.

Gosche, K.M., Mortimer, J.A., Smith, C.D., Markesbery, W.R., Snowdon, D.A., 2002. Hippocampal volume as an index of Alzheimer neuropathology: findings from the Nun Study. Neurology 58, 1476–1482.

Hashimoto, M., Kazui, H., Matsumoto, K., Nakano, Y., Yasuda, M., Mori, E., 2005. Does donepezil treatment slow the progression of hippocampal atrophy in patients with Alzheimer's disease? Am. J. Psychiatry 162, 676–682.

Henneman, W.J., Sluimer, J.D., Barnes, J., van der Flier, W.M., Sluimer, I.C., Fox, N.C., Scheltens, P., Vrenken, H., Barkhof, F., 2009. Hippocampal atrophy rates in Alzheimer disease: added value over whole brain volume measures. Neurology 72, 999–1007.

Herukka, S.K., Pennanen, C., Soininen, H., Pirttilä, T., 2008. CSF Abeta42, tau and phosphorylated tau correlate with medial temporal lobe atrophy. J. Alzheimers Dis. 14, 51–57.

Hinrichs, C., Singh, V., Mukherjee, L., Xu, G., Chung, M.K., Johnson, S.C., Alzheimer's Disease Neuroimaging Initiative, 2009. Spatially augmented LPboosting for AD classification with evaluations on the ADNI dataset. Neuroimage 48, 138–149.

Holland, D., Brewer, J.B., Hagler, D.J., Fennema-Notestine, C., Dale, A.M., Alzheimer's Disease Neuroimaging Initiative, 2009. Subregional neuroanatomical change as a biomarker for Alzheimer's disease. Proc. Natl. Acad. Sci. U. S. A. 106, 20954–20959.

Hua, X., Hibar, D.P., Lee, S., Toga, A.W., Jack, C.R., Jr., Weiner, M.W., Thompson, P.M., 2010. Sex and age differences in brain atrophic rates: an ADNI study with N=1368 MRI scans. Neurobiol. Aging 31, 1463–1480.

Hua, X., Leow, A.D., Lee, S., Klunder, A.D., Toga, A.W., Lepore, N., Chou, Y.Y., Brun, C., Chiang, M.C., Barysheva, M., Jack, C.R., Jr., Bernstein, M.A., Britson, P.J., Ward, C.P., Whitwell, J.L., Borowski, B., Fleisher, A.S., Fox, N.C., Boyes, R.G., Barnes, J., Harvey, D., Kornak, J., Schuff, N., Boreta, L., Alexander, G.E., Weiner, M.W., Thompson, P.M., Alzheimer's Disease Neuroimaging Initiative, 2008. 3D characterization of brain atrophy in Alzheimer's disease and mild cognitive impairment using tensor-based morphometry. NeuroImage. 41, 19–34.

Jack, C.R., Jr., Dickson, D.W., Parisi, J.E., Xu, Y.C., Cha, R.H., O'Brien, P.C., Edland, S.D., Smith, G.E., Boeve, B.F., Tangalos, E.G., Kokmen, E., Petersen, R.C., 2002. Antemortem MRI findings correlate with hippocampal neuropathology in typical aging and dementia. Neurology 58, 750–757.

Jack, C.R., Jr., Knopman, D.S., Jagust, W.J., Shaw, L.M., Aisen, P.S., Weiner, M.W., Petersen, R.C., Trojanowski, J.Q., 2010a. Hypothetical model of dynamic biomarkers of the Alzheimer's pathological cascade. Lancet Neurol. 9, 119–128.

Jack, C.R., Jr., Lowe, V.J., Weigand, S.D., Wiste, H.J., Senjem, M.L., Knopman, D.S., Shiung, M.M., Gunter, J.L., Boeve, B.F., Kemp, B.J., Weiner, M., Petersen, R.C., 2009. Serial PIB and MRI in normal, mild cognitive impairment and Alzheimer's disease: implications for sequence of pathological events in Alzheimer's disease. Brain 132, 1355–1365.

Jack, C.R., Jr., Petersen, R.C., Grundman, M., Jin, S., Gamst, A., Ward, C.P., Sencakova, D., Doody, R.S., Thal, L.J., Members of the Alzheimer's Disease Cooperative Study (ADCS), 2008. Longitudinal MRI findings from the vitamin E and donepezil treatment study for MCI. Neurobiol. Aging 29, 1285–1295.

Jack, C.R., Jr., Petersen, R.C., O'Brien, P.C., Tangalos, E.G., 1992. MR-based hippocampal volumetry in the diagnosis of Alzheimer's disease. Neurology 42, 183–188.

Jack, C.R., Jr., Petersen, R.C., Xu, Y., O'Brien, P.C., Smith, G.E., Ivnik, R.J., Boeve, B.F., Tangalos, E.G., Kokmen, E., 2000. Rates of hippocampal atrophy correlate with change in clinical status in aging and AD. Neurology 55, 484–489.

Jack, C.R., Jr., Petersen, R.C., Xu, Y.C., O'Brien, P.C., Smith, G.E., Ivnik, R.J., Boeve, B.F., Waring, S.C., Tangalos, E.G., Kokmen, E., 1999. Prediction of AD with MRI-based hippocampal volume in mild cognitive impairment. Neurology 52, 1397–1403.

Jack, C.R., Jr., Shiung, M.M., Weigand, S.D., O'Brien, P.C., Gunter, J.L., Boeve, B.F., Knopman, D.S., Smith, G.E., Ivnik, R.J., Tangalos, E.G., Petersen, R.C., 2005. Brain atrophy rates predict subsequent clinical conversion in normal elderly and amnestic MCI. Neurology 65, 1227–1231.

Jack, C.R., Jr., Slomkowski, M., Gracon, S., Hoover, T.M., Felmlee, J.P., Stewart, K., Xu, Y., Shiung, M., O'Brien, P.C., Cha, R., Knopman, D., Petersen, R.C., 2003. MRI as a biomarker of disease progression in a therapeutic trial of milameline for AD. Neurology 60, 253–260.

Jack, C.R., Jr., Wiste, H.J., Vemuri, P., Weigand, S.D., Senjem, M.L., Zeng, G., Bernstein, M.A., Gunter, J.L., Pankratz, V.S., Aisen, P.S., Weiner, M.W., Petersen, R.C., Shaw, L.M., Trojanowski, J.Q., Knopman, D.S., 2010b. Brain beta-amyloid measure and magnetic resonance imaging atophy both predict time-to-progression from mild cognitive impairment to Alzheimer's disease. Brain 133, 3336–3348.

Jagust, W.J., Zheng, L., Harvey, D.J., Mack, W.J., Vinters, H.V., Weiner, M.W., Ellis, W.G., Zarow, C., Mungas, D., Reed, B.R., Kramer, J.H., Schuff, N., DeCarli, C., Chui, H.C., 2008. Neuropathological basis of magnetic resonance images in aging and dementia. Ann. Neurol. 63, 72–80.

Kantarci, K., Petersen, R.C., Boeve, B.F., Knopman, D.S., Weigand, S.D., O'Brien, P.C., Shiung, M.M., Smith, G.E., Ivnik, R.J., Tangalos, E.G., Jack, C.R., Jr., 2005. DWI predicts future progression to Alzheimer disease in amnestic mild cognitive impairment. Neurology 64, 902–904.

Killiany, R.J., Gomez-Isla, T., Moss, M., Kikinis, R., Sandor, T., Jolesz, F., Tanzi, R., Jones, K., Hyman, B.T., Albert, M.S., 2000. Use of structural magnetic resonance imaging to predict who will get Alzheimer's disease. Ann. Neurol. 47, 430–439.

Killiany, R.J., Hyman, B.T., Gomez-Isla, T., Moss, M.B., Kikinis, R., Jolesz, F., Tanzi, R., Jones, K., Albert, M.S., 2002. MRI measures of entorhinal cortex vs hippocampus in preclinical. Adv. Neurol. 58, 1188–1196.

Kloppel, S., Stonnington, C.M., Chu, C., Draganski, B., Scahill, R.I., Rohrer, J.D., Fox, N.C., Jack, C.R., Jr., Ashburner, J., Frackowiak, R.S., 2008. Automatic classification of MR scans in Alzheimer's disease. Brain 131, 681–689.

Kohannim, O., Hua, X., Hibar, D.P., Lee, S., Chou, Y.-Y., Toga, A.W., Jack, C.R., Jr., Weiner, M.W., Thompson, P.M., 2010. Boosting power for clinical trials using classifiers based on multiple biomarkers. Neurobiol. Aging 31, 1429–1442.

Krishnan, K.R., Charles, H.C., Doraiswamy, P.M., Mintzer, J., Weisler, R., Yu, X., Perdomo, C., Ieni, J.R., Rogers, S., 2003. Randomized, placebo-controlled trial of the effects of donepezil on neuronal markers and hippocampal volumes in Alzheimer's disease. Am. J. Psychiatry 160, 2003–2011.

Landau, S.M., Harvey, D., Madison, C.M., Reiman, E.M., Foster, N.L., Aisen, P.S., Petersen, R.C., Shaw, L.M., Trojanowski, J.Q., Jack, C.R., Jr., Weiner, M.W., Jagust, W.J., Alzheimer's Disease Neuroimaging Initiative, 2010. Comparing predictors of conversion and decline in mild cognitive impairment. Neurology 75, 230–238.

Leung, K.K., Clarkson, M.J., Bartlett, J.W., Clegg, S., Jack, C.R., Jr., Weiner, M.W., Fox, N.C., Ourselin, S., Alzheimer's Disease Neuroimaging Initiative, 2010. Robust atrophy rate measurement in Alzheimer's disease using multi-site serial MRI: Tissue-specific intensity normalization and parameter selection. Neuroimage 50, 516–523.

McEvoy, L.K., Fennema-Notestine, C., Roddey, J.C., Hagler, D.J., Jr., Holland, D., Karow, D.S., Pung, C.J., Brewer, J.B., Dale, A.M., Alzheimer's Disease Neuroimaging Initiative, 2009. Alzheimer disease: quantitative structural neuroimaging for detection and prediction of clinical and structural changes in mild cognitive impairment. Radiology 251, 195–205.

Petersen, R.C., 2004. Mild cognitive impairment as a diagnostic entity. J. Intern. Med. 256, 183–194.

Petersen, R.C., 2007. Mild cognitive impairment. Continuum lifelong learning. Neurologist 13, 15–38.

Risacher, S.L., Saykin, A.J., West, J.D., Shen, L., Firpi, H.A., McDonald, B.C., Alzheimer's Disease Neuroimaging Initiative (ADNI), 2009. Baseline MRI predictors of conversion from MCI to probable AD in the ADNI cohort. Curr. Alzheimer Res. 6, 347–361.

Scheltens, P., Leys, D., Barkhof, F., Huglo, D., Weinstein, H.C., Vermersch, P., Kuiper, M., Steinling, M., Wolters, E.C., Valk, J., 1992. Atrophy of medial temporal lobes on MRI in "probable" Alzheimer's disease and normal ageing: diagnostic value and neuropsychological correlates. J. Neurol. Neurosurg. Psychiatry 55, 967–972.

Schott, J.M., Frost, C., Whitwell, J.L., Macmanus, D.G., Boyes, R.G., Rossor, M.N., Fox, N.C., 2006. Combining short interval MRI in Alzheimer's disease: Implications for therapeutic trials. J. Neurol. 253, 1147–1153.

Schuff, N., Woerner, N., Boreta, L., Kornfield, T., Shaw, L.M., Trojanowski, J.Q., Thompson, P.M., Jack, C.R., Jr., Weiner, M.W., 2009. MRI of hippocampal volume loss in early Alzheimer's disease in relation to ApoE genotype and biomarkers. Brain 132, 1067–1077.

Silbert, L.C., Quinn, J.F., Moore, M.M., Corbridge, E., Ball, M.J., Murdoch, G., Sexton, G., Kaye, J.A., 2003. Changes in premorbid brain volume predict Alzheimer's disease pathology. Neurology 61, 487–492.

Stonnington, C.M., Tan, G., Klöppel, S., Chu, C., Draganski, B., Jack, C.R., Jr., Chen, K., Ashburner, J., Frackowiak, R.S., 2008. Interpreting scan data acquired from multiple scanners: a study with Alzheimer's disease. Neuroimage 39, 1180–1185.

Stoub, T.R., Rogalski, E.J., Leurgans, S., Bennett, D.A., deToledo-Morrell, L., 2010. Rate of entorhinal and hippocampal atrophy in incipient and mild AD: relation to memory function. Neurobiol. Aging 31, 1089–1098.

Tapiola, T., Pennanen, C., Tapiola, M., Tervo, S., Kivipelto, M., Hänninen, T., Pihlajamäki, M., Laakso, M.P., Hallikainen, M., Hämäläinen, A., Vanhanen, M., Helkala, E.L., Vanninen, R., Nissinen, A., Rossi, R., Frisoni, G.B., Soininen, H., 2008. MRI of hippocampus and entorhinal cortex in mild cognitive impairment: a follow-up study. Neurobiol. Aging 29, 31–38.

Thompson, P.M., Apostolova, L.G., 2007. Computational anatomical methods as applied to ageing and dementia. Br. J. Radiol. 80(Spec 2):S78–91.

Tzourio-Mazoyer, N., Landeau, B., Papathanassiou, D., Crivello, F., Etard, O., Delcroix, N., Mazoyer, B., Joliot, M., 2002. Automated anatomical labeling of activations in SPM using a macroscopic anatomical parcellation of the MNI MRI single-subject brain. Neuroimage 15, 273–289.

Vemuri, P., Gunter, J.L., Senjem, M.L., Whitwell, J.L., Kantarci, K., Knopman, D.S., Boeve, B.F., Petersen, R.C., Jack, C.R., Jr., 2008a. Alzheimer's disease diagnosis in individual subjects using structural MR images: validation studies. Neuroimage 39, 1186–1197.

Vemuri, P., Jack, C.R., Jr., 2010. Role of structural MRI in Alzheimer's disease. Alzheimers Res. Ther. 2, 23.

Vemuri, P., Whitwell, J.L., Kantarci, K., Josephs, K.A., Parisi, J.E., Shiung, M.S., Knopman, D.S., Boeve, B.F., Petersen, R.C., Dickson, D.W., Jack, C.R., Jr., 2008b. Ante mortem MRI based STructural Abnormality iNDex (STAND)-scores correlate with postmortem Braak neurofibrillary tangle stage. Neuroimage 42, 559–567.

Vemuri, P., Wiste, H.J., Weigand, S.D., Knopman, D.S., Trojanowski, J.Q., Shaw, L.M., Bernstein, M.A., Aisen, P.S., Weiner, M., Petersen, R.C., Jack, C.R., Jr., Alzheimer's Disease Neuroimaging Initiative, D.N., 2010. Serial MRI and CSF biomarkers in normal aging, MCI, and AD. Neurology 75, 143–151.

Vemuri, P., Wiste, H.J., Weigand, S.D., Shaw, L.M., Trojanowski, J.Q., Weiner, M.W., Knopman, D.S., Petersen, R.C., Jack, C.R., Jr., Alzheimer's Disease Neuroimaging Initiative, 2009. MRI and CSF biomarkers in normal, MCI, and AD subjects: Predicting future clinical change. Neurology 73, 294–301.

Visser, P.J., Krabbendam, L., Verhey, F.R., Hofman, P.A., Verhoeven, W.M., Tuinier, S., Wester, A., Den Berg, Y.W., Goessens, L.F., Werf, Y.D., Jolles, J., 1999. Brain correlates of memory dysfunction in alcoholic Korsakoff's syndrome. J. Neurol. Neurosurg., Psychiatry 67, 774–778.

Visser, P.J., Verhey, F.R., Hofman, P.A., Scheltens, P., Jolles, J., 2002. Medial temporal lobe atrophy predicts Alzheimer's disease in patients with minor cognitive impairment. J. Neurol. Neurosurg. Psychiatry 72, 491–497.

Walhovd, K.B., Fjell, A.M., Brewer, J., McEvoy, L.K., Fennema-Notestine, C., Hagler, D.J., Jr., Jennings, R.G., Karow, D., Dale, A.M., Alzheimer's Disease Neuroimaging Initiative, 2010. Combining MR imaging, positron-emission tomography, and CSF biomarkers in the diagnosis and prognosis of Alzheimer disease. AJNR Am. J. Neuroradiol. 31, 347–354.

Wang, P.N., Liu, H.C., Lirng, J.F., Lin, K.N., Wu, Z.A., 2009. Accelerated hippocampal atrophy rates in stable and progressive amnestic mild cognitive impairment. Psychiatry Res. 171, 221–231.

Welch, E.B., Manduca, A., Grimm, R.C., Ward, H.A., Jack, C.R., Jr., 2002. Spherical navigator echoes for full 3-D rigid body motion measurement in MRI. Mag Reson Med. 47(1), 32–41.

Whitwell, J.L., Josephs, K.A., Murray, M.E., Kantarci, K., Przybelski, S.A., Weigand, S.D., Vemuri, P., Senjem, M.L., Parisi, J.E., Knopman, D.S., Boeve, B.F., Petersen, R.C., Dickson, D.W., Jack, C.R., Jr., 2008. MRI correlates of neurofibrillary tangle pathology at autopsy: a voxel-based morphometry study. Neurology 71, 743–749.

Whitwell, J.L., Przybelski, S.A., Weigand, S.D., Knopman, D.S., Boeve, B.F., Petersen, R.C., Jack, C.R., Jr., 2007. 3D maps from multiple MRI illustrate changing atrophy patterns as subjects progress from mild cognitive impairment to Alzheimer's disease. Brain 130, 1777–1786.

Wolz, R., Heckemann, R.A., Aljabar, P., Hajnal, J.V., Hammers, A., Lötjönen, J., Rueckert, D., Alzheimer's Disease Neuroimaging Initiative, 2010. Measurement of hippocampal atrophy using 4D graph-cut segmentation: application to ADNI. Neuroimage 52, 109–118.

Xu, Y., Jack, C.R., Jr., O'Brien, P.C., Kokmen, E., Smith, G.E., Ivnik, R.J., Boeve, B.F., Tangalos, R.G., Petersen, R.C., 2000. Usefulness of MRI measures of entorhinal cortex versus hippocampus in AD. Neurology 54, 1760–1767.

Zarow, C., Vinters, H.V., Ellis, W.G., Weiner, M.W., Mungas, D., White, L., Chui, H.C., 2005. Correlates of hippocampal neuron number in Alzheimer's disease and ischemic vascular dementia. Ann. Neurol. 57, 896–903.